Electronic Supplementary Information for

High Electroactive Material Loading on a Carbon Nanotube/Carbon Nanofiber as Advanced Free-Standing Electrode for Asymmetric Supercapacitors

Yongsheng Zhou [,a,b], Yingchun Zhu [b], Bingshe Xu [c], and Xueji Zhang [*,d]*

[a]College of Chemistry and Materials Engineering, Anhui Science and Technology University, Bengbu, 233030, P. R. China

[b]Key Laboratory of Inorganic Coating Materials CAS, Shanghai Institute of Ceramics, Chinese Academy of Sciences, Shanghai, 200050, P. R. China

[c]Key Laboratory of Interface Science and Engineering in Advanced Materials, Ministry of Education, Taiyuan University of Technology, Taiyuan, 030024, P. R. China

[d]Beijing Key Laboratory for Bioengineering and Sensing Technology, Research Center for Bioengineering and Sensing Technology, School of Chemistry and Bioengineering, University of Science & Technology Beijing, 30 Xueyuan Road, Haidian District, Beijing 100083, P. R. China

E-mail: yszhou1981@gmail.com; E-mail: zhangxueji@ustb.edu.cn

Experimental section

Preparation of Co_9S_8@CNT/CNF

For the growth of Co_9S_8@CNT/CNF, a gel precursor was first prepared by dissolving $Co(AC)_2 \cdot 4H_2O$ (Ac = acetate) (1.0 g), polyacrylonitrile (PAN) (0.1 g), polyethylene glycol (PEG) (2.5 g), and C_2H_6S (10 ml) in 10 mL ethanol under vigorous stirring for 3 h, followed by gelation at 40 °C for 8 h and heating at 100 °C for 4 h. Co_9S_8@CNT/CNF was grown on the resulting xerogel at 1,000 °C under a gas flow with $Ar:C_2H_4:H_2$ =300:10:20 sccm (standard-state cubic centimeter per minute) in a horizontal tube furnace.

Preparation of Co_9S_8@CNT

The Co_9S_8@CNT material was prepared in a way similar to that for the Co_9S_8@CNT/CNF material, but C_2H_4 was not added to the reaction.

Preparation of CNT/CNF

The CNTs/CNFs was harvested after the acidic etching of the sample by a hot concentrated HNO_3 solution to remove Co_9S_8.

Characterization of materials

Scanning electron microscope (SEM) images were obtained using an S-4800 field emission scanning electron microscope (Hitachi, Japan) operating at 10 kV. Transmission electron microscope (TEM) images were obtained using a FEI Titan G2 60-300 operating at 80 kV. The X-ray diffraction (XRD) patterns were measured on a Shimadzu XRD-7000 X-ray diffractometer. N_2 sorption analysis was conducted on an ASAP2020 accelerated surface area and porosimetry instrument (Micromeritics), equipped with automated surface area, at 77 K using BarrettEmmettTeller (BET) calculations for the surface area. The pore size distribution (PSD) plot

was recorded from the adsorption branch of the isotherm based on the density functional theory (DFT) model.

Electrochemical measurements

For electrochemical measurements, the working electrode was prepared by mixing the electroactive material, carbon black (super-P-Li) and polymer binder (polyvinylidene difluoride) in a weight ratio of 70:20:10. The slurry was pressed onto Ni foam and dried at 90 ℃ for 10 h. Electrochemical measurements were conducted with a CHI 660C electrochemical workstation in an aqueous KOH electrolyte (2.0 M) with a three-electrode cell where a Pt foil serves as the counter electrode and a saturated calomel electrode as the reference electrode. The tap density of the Co_9S_8@CNT/CNF was estimated by directly measuring the mass and physical dimensions occupied, which is about 0.5 g cm^{-3}. The mass loading of Co_9S_8@CNT/CNF is about 5 mg cm^{-2}.

The electrochemical performances of the asymmetric supercapacitor (ASC) were measured by two-electrode system. The optimized mass ratio of the positive electrode and negative electrode is 0.3. The active masses in the positive electrode were 3 mg and the active masses in the negative electrode were 10 mg, respectively.

The specific capacitance (C) is calculated from CV and GCD curves by following equation:

$$C = \frac{\int Idv}{S \bullet \Delta V \bullet m} \qquad (1)$$

$$C_{sp} = \frac{I \Delta t}{m \Delta V} \qquad (2)$$

where I is the current used for charge/discharge in A, S is the scan rate in V s^{-1}, Δt is the time elapsed for the discharge cycle in s, m is the mass of the active electrode material in g, and ΔV is the voltage interval of the charge or discharge in V.

The energy density (E) and power density (P) of ASCs against the two electrodes in device were calculated based on the total mass of the active materials using the following equations:

$$E_d = \frac{1}{2}C_{sp}\Delta V^2 \qquad (3)$$

$$P_d = \frac{E_d}{\Delta t} \qquad (4)$$

where C_{sp} is the specific capacitance, ΔV is the voltage change of the supercapacitor between completely charged and discharged, and Δt is the discharge time.
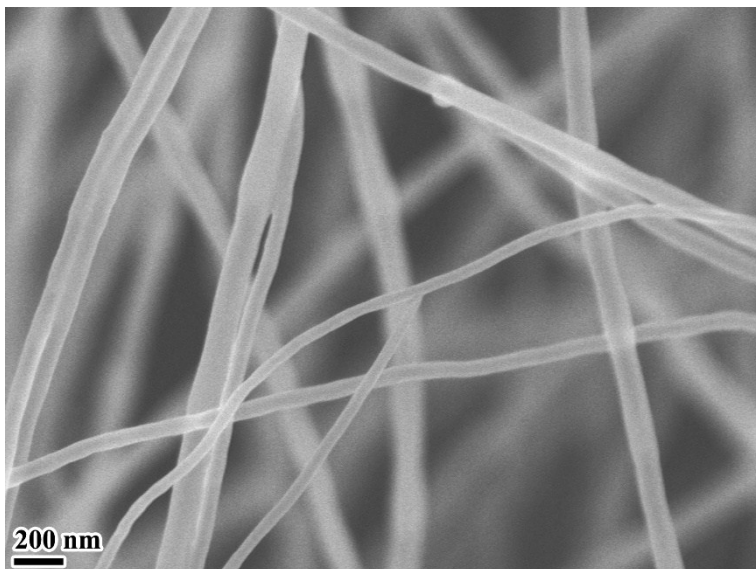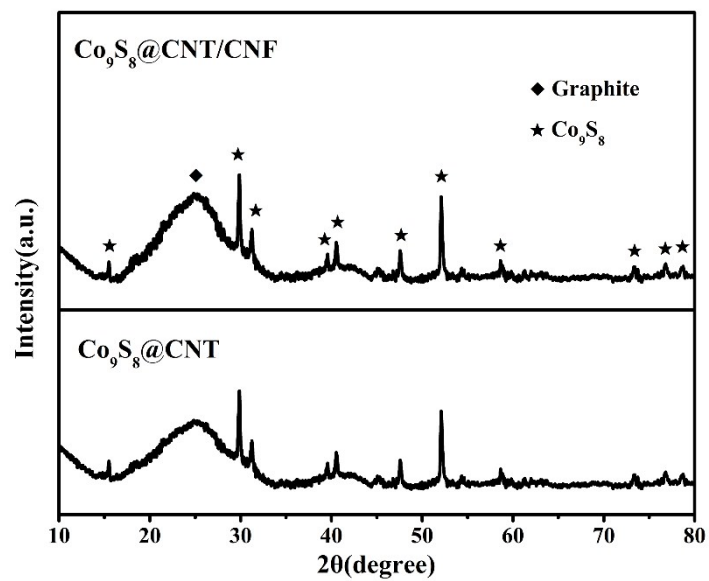
Figure S1. SEM image of $Co_9S_8@CNT$.

Figure S2. XRD spectroscopic of the Co_9S_8@CNT/CNF and Co_9S_8@CNT.
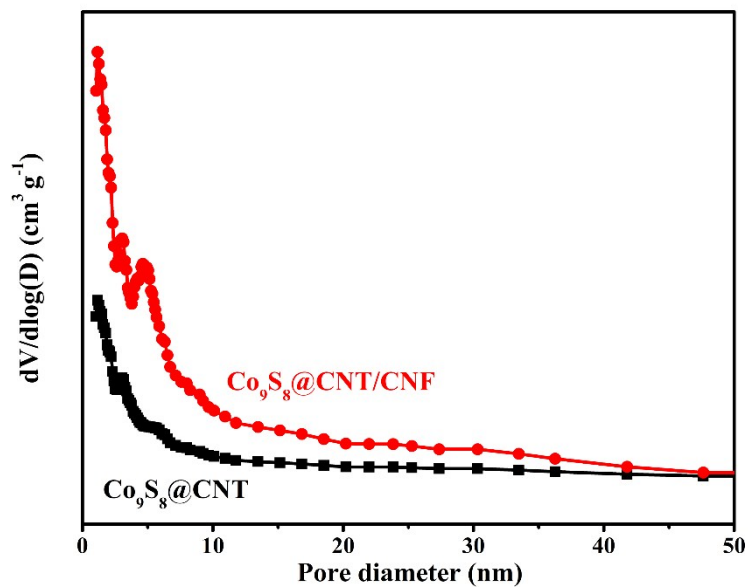
Figure S3. Pore size distributions of Co_9S_8@CNT/CNF and Co_9S_8@CNT.

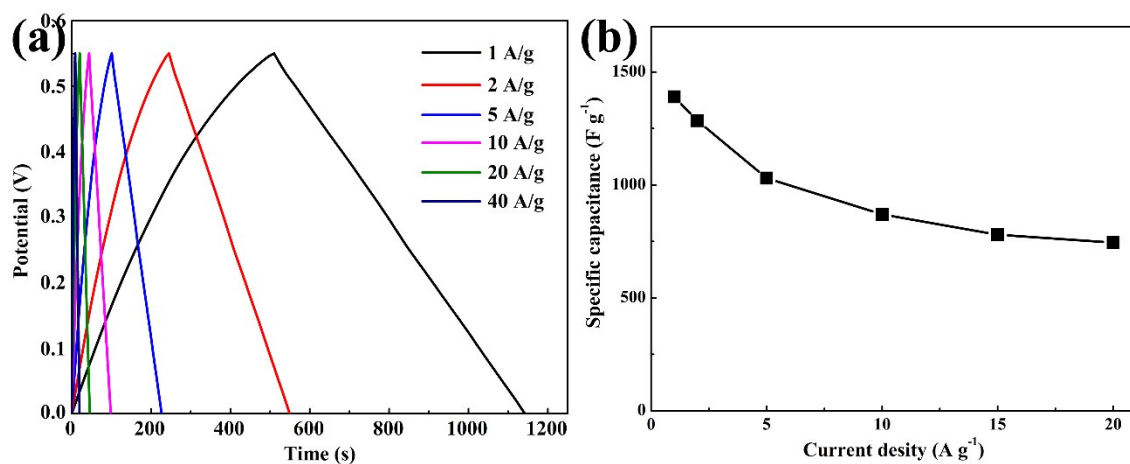**Figure S4.** Electrochemical characterizations of the Co_9S_8@CNT electrode. (a) Galvanostatic charge/discharge voltage profiles; (b) specific capacitance as a function of current density.

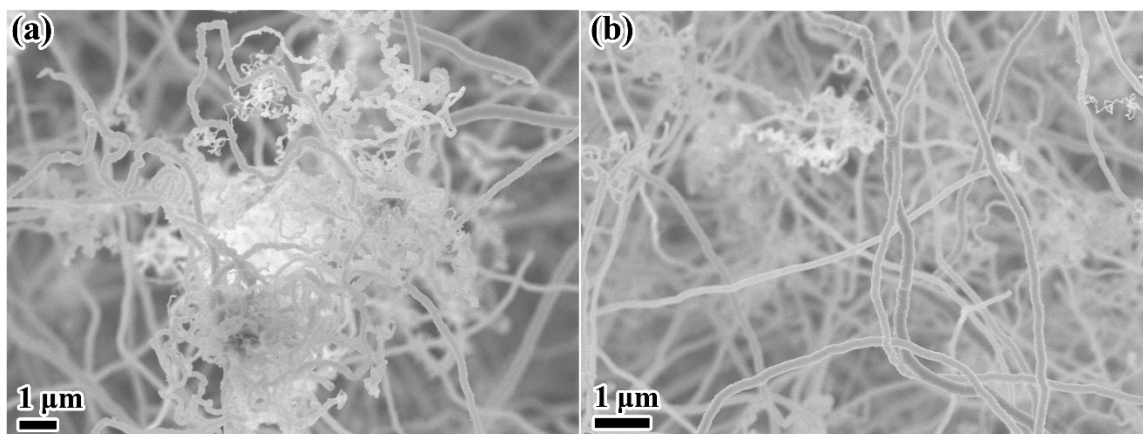**Figure S5.** SEM images of Co$_9$S$_8$@CNT/CNF before (a) and after (b) 5 000 cycling tests.
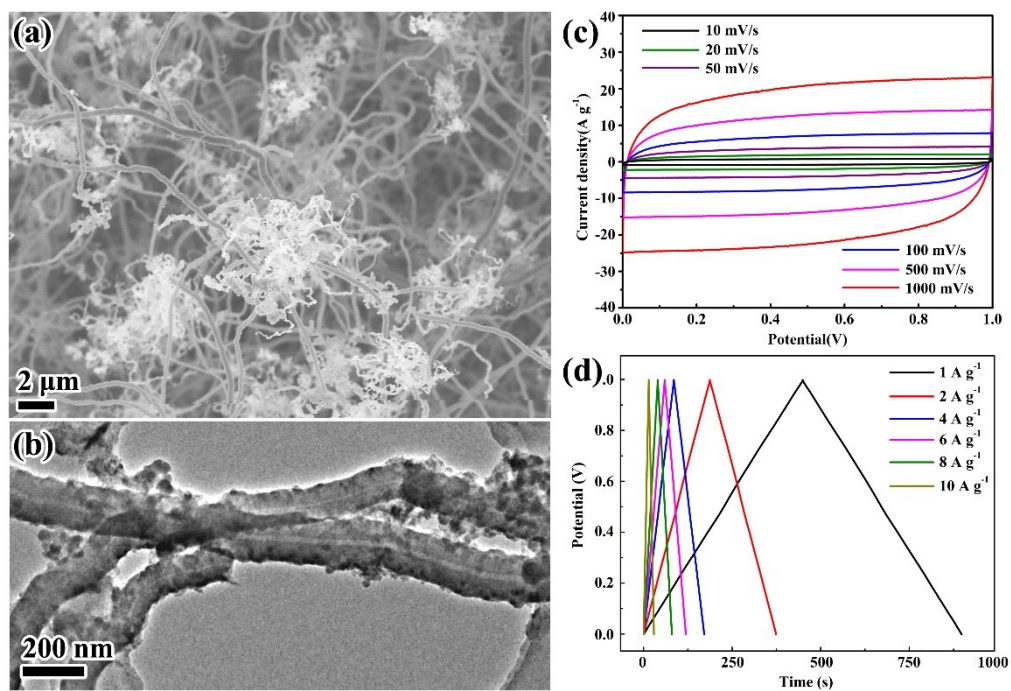
Figure S6. Microstructure and electrochemical performance of CNT/CNF. (a) FESEM image of CNT/CNF. (b) TEM image of CNT/CNF. (c) CV curves at various scan rates from 10 to 1000 mV s^{-1}. (d) Galvanostatic charge/discharge voltage profiles at different current densities.

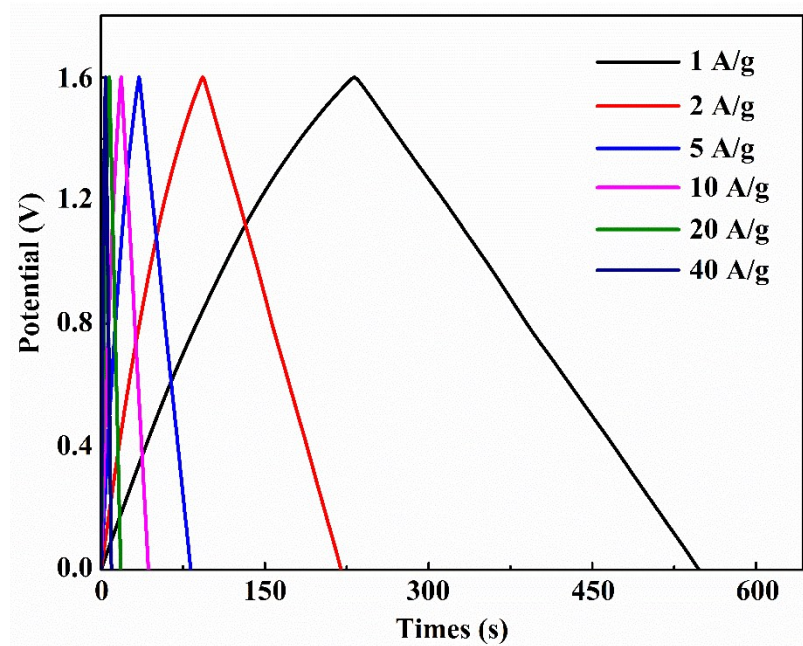**Figure S7.** Galvanostatic charge/discharge voltage profiles of the ASC device at different current densities from 1 to 40 A g^{-1}.
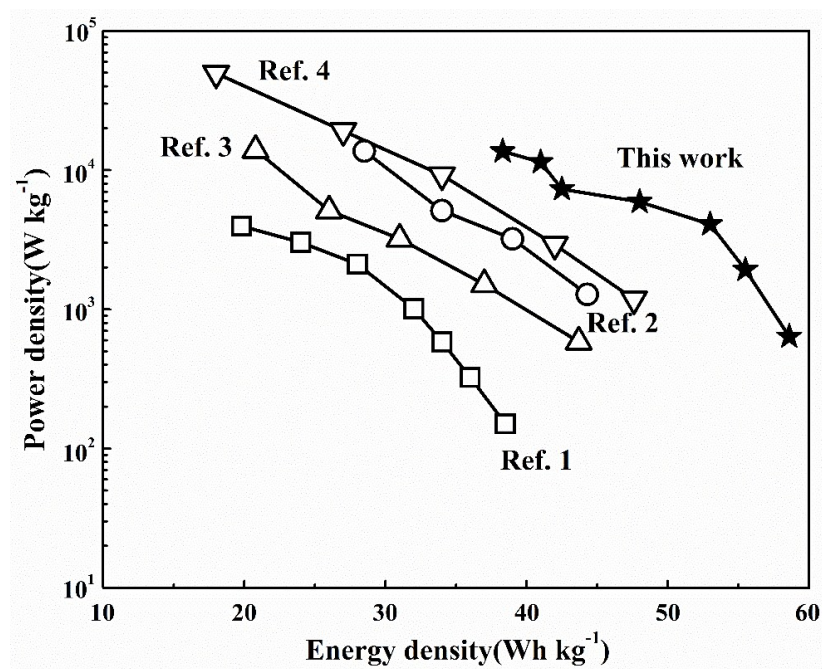
Figure S8. Ragone plots of ASC devices. The reported values for other ASC devices are added for comparison.

Table S1| Specific capacitance values of different metals sulfides -based materials for

Materials	mass loading	Current density	Specific Capacity	References
$Ni_xCo_{9-x}S_8$@C	4 mg cm^{-2}	2 A g^{-1}	1404 F g^{-1}	5
rGO/CoNiS$_x$/N–C	3 mg	1 A g^{-1}	1028.2 F g^{-1}	6
Co$_9$S$_8$-NSA/NF	N/A	0.5 A g^{-1}	1098.8 F g^{-1}	7
NiCo$_2$S$_4$@G	N/A	1 A g^{-1}	1432 F g^{-1}	8
H-3DRG@NiCo$_2$S$_4$	N/A	1 A g^{-1}	783 F g^{-1}	9
Co$_3$S$_4$ nanospheres/ graphene	N/A	5 A g^{-1}	522 F g^{-1}	10
NiS/rGO composite	N/A	5 A g^{-1}	579 F g^{-1}	11
NiCo$_2$S$_4$ nanosheets/graphene	N/A	20 A g^{-1}	760 F g^{-1}	12
CoS	0.283 mg cm^{-2}	1 A g^{-1}	224 F g^{-1}	13
NiCo$_2$S$_4$	5 mg cm^{-2}	1 A g^{-1}	1036 F g^{-1}	14
NiCo$_2$S$_4$ nanotube	1.2 mg	5 A g^{-1}	550 F g^{-1}	15
NiCo$_2$S$_4$ nanoplates	N/A	20 A g^{-1}	231 F g^{-1}	16
NiCo$_2$S$_4$ nanoprisms	1.7 mg cm^{-2}	20 A g^{-1}	585 F g^{-1}	17
NiCo$_2$S$_4$ mesoporous nanoparticles	N/A	20 A g^{-1}	840 F g^{-1}	18
Our work	5 mg cm^{-2}	1 A g^{-1}	1580 F g^{-1}	

supercapacitors.

References

1. S. Dai, B. Zhao, C. Qu, D. Chen, D. Dang, B. Song, B. M. Deglee, J. Fu, C. Hu, C.-P. Wong, M. Liu, Nano Energy **2017**, 33, 522.

2. J. Yang, C. Yu, X. Fan, S. Liang, S. Li, H. Huang, Z. Ling, C. Hao, J. Qiu, Energy Environ. Sci. **2016**, 9, 1299;

3. H. Hu, B. Y. Guan, X. W. Lou, Chem **2016**, 1, 102

4. Y. Zhang, L. Zuo, L. Zhang, J. Yan, H. Lu, W. Fan, T. Liu, Nano Res. **2016**, 9, 2747.

5. Y. Zhang, C. Sun, H. Su, W. Huang, X. Dong, Nanoscale **2015**, 7, 3155.

6. Q. Chen, J. Miao, L. Quan, D. Cai, H. Zhan, Nanoscale **2018**, 10, 4051.

7. X. Han, K. Tao, D. Wang, L. Han, Nanoscale **2018**, 10, 2735.

8. F. Yu, Z. Chang, X. Yuan, F. Wang, Y. Zhu, L. Fu, Y. Chen, H. Wang, Y. Wu, W. Li, J. Mater. Chem. A **2018**, 6, 5856.

9. K. Qin, L. Wang, S. Wen, L. Diao, P. Liu, J. Li, L. Ma, C. Shi, C. Zhong, W. Hu, E. Liu, N. Zhao, J. Mater. Chem. A **2018**, 6, 8109.

10. Q. H. Wang, L. F. Jiao, H. M. Du, Y. C. Si, Y. J. Wang, H. T. Yuan, J. Mater. Chem. **2012**, 22, 21387-21391.

11. J. Yang, X. Duan, W. Guo, D. Li, H. Zhang, W. Zheng, Nano Energy **2014**, 5, 74-81.

12. S. J. Peng, L. L Li, C. C. Li, H. T. Tan, R. Cai, H. Yu, S. Mhaisalkar, M. Srinivasan, S. Ramakrishna, Q. Y. Yan, Chem. Commun. **2013**, 49, 10178-10180.

13. B. You, N. Jiang, M. Sheng, Y. Sun, Chem. Commun. **2015**, 51, 4252.

14. L. Shen, L. Yu, H. B. Wu, X.-Y. Yu, X. Zhang, X. W. Lou, Nat. Commun. **2015**, 6.

15. H. Z. Wan, J. J. Jiang, J. W. Yu, K. Xu, L. Miao, L. Zhang, H. C. Chen, Y. J. Ruan. CrystEngComm **2013**, 15, 7649-7651.

16. J. Pu, F. L. Cui, S. B. Chu, T. L. Wang, E. H. Sheng, Z. H. Wang, ACS Sustainable Chem. Eng. **2014**, 2, 809-815.

17. L. Yu, L. Zhang, H. B. Wu, X. W. Lou, Angew. Chem. Int. Ed. **2014**, 53, 3711-3714.

18. Y. R. Zhu, Z. B. Wu, M. J. Jing, X. M. Yang, W. X. Song, X. B. Ji, J. Power Sources **2015**, 273, 584-590.